

The Influence of Ocean Surface Temperature Gradient and Continentality on the Walker Circulation. Part I: Prescribed Tropical Changes

ROBERT M. CHERVIN

National Center for Atmospheric Research,¹ Boulder, CO 80307

LEONARD M. DRUYAN²

NASA/Goddard Institute for Space Studies, Goddard Space Flight Center, New York, NY 10025

(Manuscript received 16 December 1983, in final form 25 April 1984)

ABSTRACT

A coarse-mesh, global climate model developed at the Goddard Institute for Space Studies (GISS) has been used to assess the influence of ocean surface temperature (OST) gradient and continentality on the Walker circulation. The basic model climate was established by a five-year integration in which the prescribed seasonal cycle in OST distribution was identical for each year. In the model climate, the Walker circulation is characterized in the zonal plane by three pairs of clockwise and counterclockwise cells in the troposphere.

Three separate winter experiments were performed in which the normal west-to-east OST gradients in the tropical Pacific were replaced by a uniform distribution in the band from 8°N to 16°S. Each experiment was characterized by OSTs set at the warmest, coldest, or mean temperatures in the band. The model response features statistically significant changes in the intensity of the various cells and branches with small shifts in the east-west extent. The overall structure in the zonal plane for the experiments with the coldest or mean temperatures, however, remained unchanged. A major disruption of the six-cell structure did result for the experiment with the warmest temperature and resultant net heat source.

The fourth prescribed changed experiment involved the replacement of the South American continent by an ocean with the OSTs linearly interpolated from the eastern Pacific to the western Atlantic. In this case, a dramatic change in the structure of the Walker circulation also took place as the upward branch over South America was reduced sufficiently to eliminate the corresponding counterclockwise cell and thereby allow two clockwise cells to merge into one large cell. The Hadley cell was less intense and shifted northward with the South American continent removed.

In summary, these experiments with the GISS model seem to indicate that both continentality and OST gradient are important as forcing mechanisms of the overall structure of the Walker circulation and the intensity of the individual cells. The details of the forcing, however, are likely to be different for the two mechanisms.

1. Introduction

The term "Walker circulation" was first defined by Bjerknes (1969) to describe an exchange of air in the zonal plane for the equatorial belt from South America to the western Pacific. Bjerknes considered this circulation to be part of the global Southern Oscillation phenomenon defined earlier in the statistical sense by Sir Gilbert Walker (1923, 1924, 1928). Bjerknes also postulated that the gradient of ocean surface temperature (OST) along the equator was the cause of the Walker circulation. Newell *et al.* (1974) later expanded this concept by considering circulations

in zonal planes circumscribing the entire globe at any tropical latitude. In this paper, we adopt this expanded conception of the Walker circulation.

Numerical experiments with general circulation models (GCMs) by Rowntree (1972) and Julian and Chervin (1978) have indicated that prescribed changes in tropical Pacific OST can affect the winds associated with the Walker circulation in the Pacific sector. However, a heat budget analysis for the Pacific Ocean near 10°S by Cornejo-Garrido and Stone (1977) suggests that the convergence of moisture above the central and western Pacific and the subsequent condensation and heating there serve as the principal driving force for maintaining the Walker circulation with OST gradients playing only a secondary role.

In this study, we examine the influence of prescribed changes of OST gradient and continentality in the tropical Pacific sector on the global Walker circulation by means of a coarse-mesh global climate model developed at the Goddard Institute for Space Studies

¹ The National Center for Atmospheric Research is sponsored by the National Science Foundation.

² Served as a Senior Resident Research Associate at NASA under the sponsorship of the National Research Council/National Academy of Sciences. On sabbatical leave during 1979–80 from Department of Geography, Bar Ilan University, Ramat Gan, Israel.

(GISS). We also consider the extratropical responses to these altered surface forcings. A companion paper by Stone and Chervin (1984) features prescribed global changes in OST gradient and continentality in order to eliminate possible forcings from outside the tropical latitudinal band in which the Walker circulation is identified.

2. Description of model and model climate

The model used in our experiments was developed by the climate research group at GISS and is comprehensively described and documented by Hansen *et al.* (1983) with the designation "Model II." An earlier version of this model ("Model I") was used by Christidis and Spar (1981) for the purpose of demonstrating the utility of verifying a simulated climate by means of a spherical harmonic analysis and by Druyan (1982a,b) for studying the Indian summer monsoon. A brief description of those features of Model II pertinent to sensitivity studies involving the Walker circulation is presented below. More complete information is available in Hansen *et al.* (1983).

Model II employs finite difference approximations to the equations of motion in spherical coordinates with sigma (i.e., normalized pressure) as the vertical coordinate. The Arakawa B grid scheme is used with a horizontal resolution of 10° in the zonal direction (36 points) and approximately 8° in the meridional direction (24 points). There are nine layers in the vertical with layer interfaces at sigma values 0.984, 0.934, 0.854, 0.720, 0.550, 0.390, 0.255, 0.150, 0.070 and 0.010 and layer "midpoints" at sigma values 0.959, 0.894, 0.786, 0.634, 0.468, 0.321, 0.201, 0.103 and 0.027. Physical processes contained in the model include solar and terrestrial radiation, vertical transport of moisture, sensible heat and momentum by convection, large-scale clouds, heat and moisture storage in the ground surface and vertical transports of latent heat, sensible heat and momentum from the surface. In particular, the convective instability process is parameterized in Model II based on moist static energy considerations in which mass is allowed to rise to the highest layer with respect to which it is buoyant, rather than to just the next higher layer. Moisture is condensed if saturation occurs and the moist static energy is conserved by the rising parcels. Mixing of mass with lower levels compensates for the mass in the rising parcels. Previously condensed moisture is permitted to reevaporate when unsaturated lower layers are encountered. This procedure starts with the lowest layer as the source of the rising parcels and then is repeated sequentially with each next higher layer as the source. The most evident consequence of employing the above convective parameterization instead of the conventional moist adiabatic adjustment scheme of Manabe *et al.* (1965) is

the achievement of a more realistic distribution of moist convective heating. Additional differences are described in Hansen *et al.* (1983). Ocean surface temperatures are prescribed and follow an annual cycle. Ocean ice, subsurface land temperature, soil moisture and snow cover are computed from energy balance and hydrological parameterizations. Both a diurnal and an annual cycle are included for the radiation calculations.

Model II was integrated for six years starting from observed data derived from the operational analyses of the National Meteorological Center (NMC). The monthly means computed from the last five model years represent a sampled climate ensemble for the model which may be used to compute estimates of ensemble statistics (Chervin, 1980a). This long-term integration serves as a control case for our subsequent sensitivity studies. Hansen *et al.* (1983) evaluated the model's simulated climate and concluded that it produces a reasonable representation of global pressure patterns, cloud and precipitation distribution and circulation.

We represent the Walker circulation simulated by the model during January by means of longitude-height cross sections averaged over the three model latitudes contained between 8°N – 16°S . This selection of a meridionally averaged measure of the model's Walker circulation was predicated on a desire to obtain representative results emphasizing the large-scale features of the phenomena within the context of a comparatively coarse resolution model which obviously cannot resolve many observed small-scale features. Such averaging also reduces the inherent variability in climate statistics (see, e.g., Chervin, 1980b). Furthermore, for the simulated fields of interest, strong inhomogeneities were not apparent in this latitudinal band. Estimates of ensemble averages and standard deviations for the zonal wind and the vertical velocity in this zonal plane are shown in Fig. 1. In the model climate, the global Walker circulation is characterized by three dipole-like features denoting an alternating pattern of westerly and easterly flow in the upper troposphere. Each of these dipoles is associated with an opposite-signed dipole in the lower troposphere. The upper and lower dipoles are connected by ascending and descending branches to form quasi-two-dimensional circulation cells in the zonal plane. The strongest ascending branch is located over South America and strong ascent is also noted over Africa. The standard deviations are included to indicate the magnitude of the unforced inherent variability in the model's January climate since each simulated January has the identical prescription of OST distribution. The maxima in the standard deviations typically correspond to the maxima in the ensemble averages or to transitions between either westerlies and easterlies or ascending and descending branches. This latter type of maxima indicates that

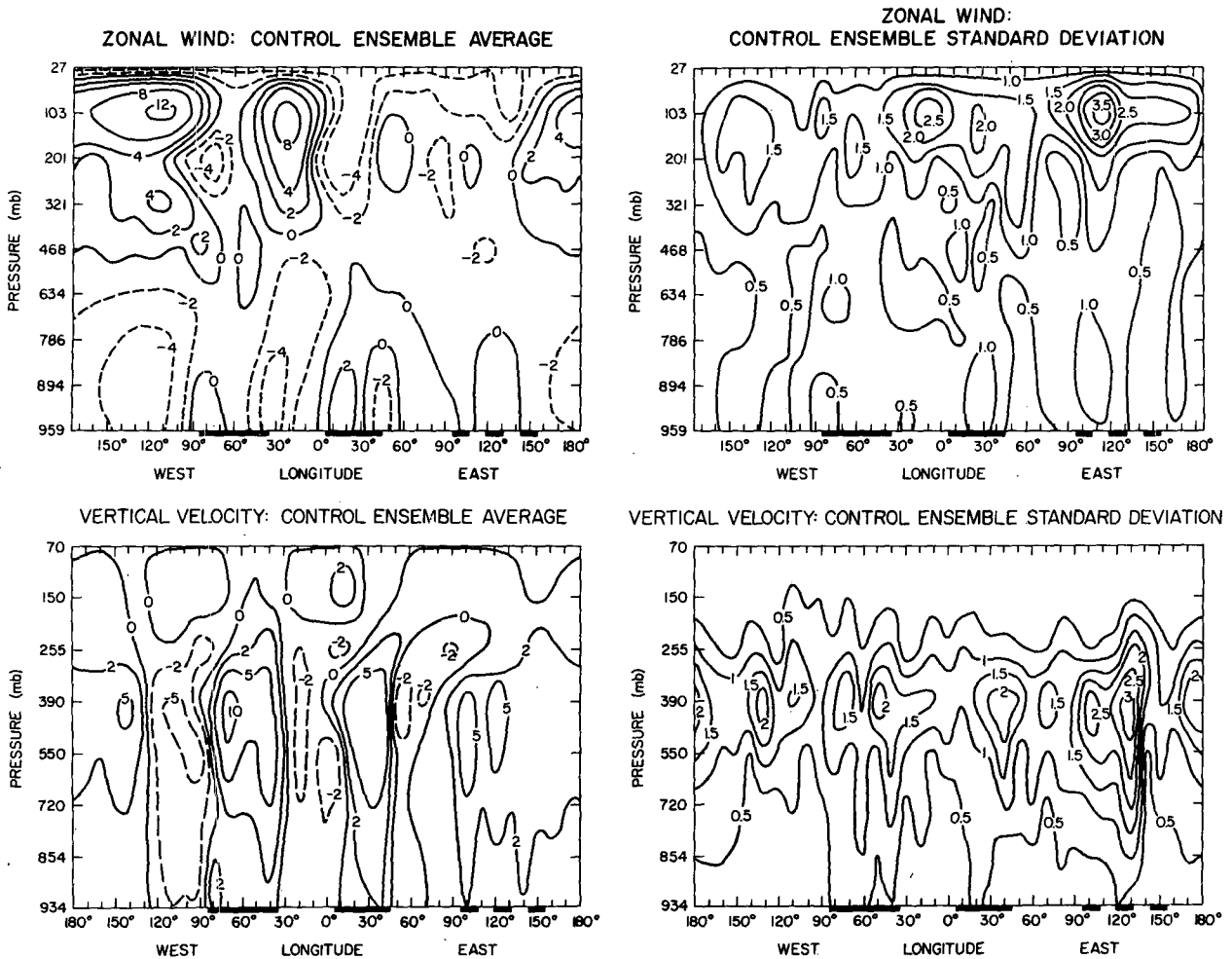


FIG. 1. The Walker circulation simulated by Model II averaged over the three model latitudes contained between 8°N and 16°S. Ensemble averages and standard deviations are estimated from five independent simulated Januaries. The solid underbars indicate the South American and African continents and the broken underbar indicates the maritime continent formed by the Indonesian Archipelago and New Guinea. Units are m s^{-1} for zonal wind and mm s^{-1} for vertical velocity. The nominal pressure levels at which the variables are computed in the model are given on the vertical axes.

the model experiences some longitudinal shifts in the structure of the Walker circulation on an interannual basis.

In summary, the simulated Walker circulation in this latitude band is composed of essentially six separate (but probably highly correlated) circulations. Each of these circulation cells shares an ascending and descending branch with the next adjacent cell to the west and east. For later reference, we identify these cells as: the Pacific Ocean clockwise (when viewed from the south) cell, the South American continent counterclockwise cell, the Atlantic Ocean clockwise cell, the African continent counterclockwise cell, the Indian Ocean clockwise cell and the maritime continent (i.e., the area centered near Indonesia) counterclockwise cell. The first of these cells—the Pacific Ocean clockwise cell—is the feature traditionally identified as the Walker circulation and is ob-

viously the dominant cell in this zonal plane in terms of both intensity and spatial scale. However, the other cells must also be considered when evaluating the forcing mechanisms of our expanded conception of a global Walker circulation. The first four of these cells (i.e., Pacific, South America, Atlantic and African) may be considered major while the last two (i.e., Indian and maritime) may be considered minor with respect to strength and general coherence of the patterns. With the exception of the Indian cell, this cellular pattern may be found in the Walker circulation schematic of Newell (1979, his Fig. 8).

Our simulated Walker circulation may be qualitatively compared to an analysis of the observed Walker circulation from eight years of data by Newell *et al.* (1974). Their Fig. 9.2 (lower left) shows the "vector wind" in longitude–pressure coordinates at 5°S for a long-term December–February average. The most

apparent differences between simulations and observations with regard to the zonal wind in this plane are found in the upper troposphere over South America and over the western Indian Ocean where the signs of the winds are reversed. The vertical velocity patterns are quite similar except for the longitude of the transition between ascent and descent in the central Pacific. Part of an explanation of these discrepancies may be attributed to the relative scarcity of observing stations in this latitude band (see Plate 2.1 of Newell *et al.*, 1972). Nevertheless, the general agreement between the observed and simulated Walker circulation encouraged us to carry out the sensitivity studies described in the next section with some assurance that the model sensitivity could bear some resemblance to the sensitivity of the real atmosphere.

Since we plan to assess the extratropical response in the model to the tropical prescribed changes primarily in terms of the meridional circulation, we show estimated ensemble average and standard deviation for January zonal-mean mass streamfunction in Fig. 2. Although observational analyses of this mass flux are notoriously imprecise (see, e.g., Starr *et al.*, 1970), it is clear that the model's Hadley cell is a reasonable representation of nature although only a very weak polar cell is apparent in the ensemble average. As with the previously discussed fields, the maxima in the standard deviation correspond to either maxima in the ensemble average or transitions between cells. The relatively large variability in the high latitudes in the Northern Hemisphere indicates that the polar cell may well be more apparent in individual Januaries.

3. Experimental design

In this paper, we analyze the model's response to four different tropical prescribed changes in boundary

or surface conditions. Each of the four sensitivity experiments started on 1 December and continued until the end of January with the particular prescribed changes held constant during the length of the integration. For any field or variable, the prescribed change response (Δ) of the model is determined by subtracting the control January ensemble average from the January average appropriate for the given prescribed change experiment. A normalized response (r) is formed by dividing Δ by the estimated standard deviation from the control population to provide an indication of the statistical significance of any apparent climate change resulting from the prescribed change in boundary conditions. For the available sample sizes, a normalized response (r) greater than 3 implies that the prescribed change and control January means come from different populations at the 5% significance level (see, e.g., Chervin and Schneider, 1976). That is, the differences may be attributed to the prescribed change and not the model's inherent variability with an error of 5% or less.

The first three experiments involved removing the normal west-to-east OST gradient in the tropical Pacific sector for grid points from 150°E to the coast of South America for the three model latitude lines between 8°N and 16°S. This latitudinal band corresponds to the one used to define the Walker circulation in Fig. 1. In each case, the OST one or two lines north and south of this band were adjusted somewhat to assure a smoother poleward gradient. In the first experiment (warm temperatures/no gradient, Case WTNG), the zonal gradient of OST was eliminated by the assignment of the warm western Pacific OST values to all the grid points for each line in the band. In some respects, this OST anomaly pattern is analogous to the situation during a positive El Niño, with anomalously warm water adjacent to the Peru coast. This anomaly pattern is also similar to the one used

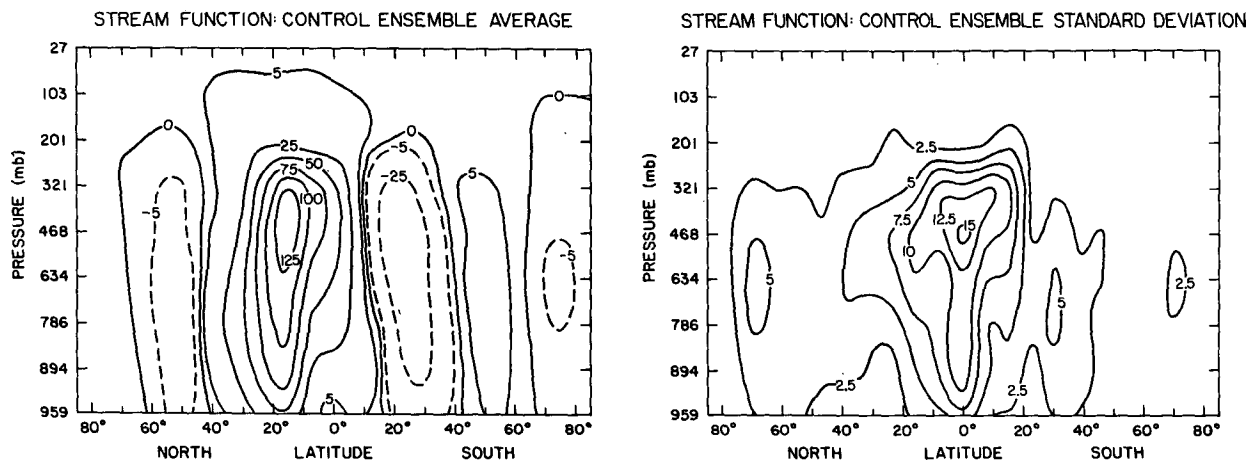


FIG. 2. The zonal-mean mass streamfunction simulated by Model II. The ensemble average and standard deviation are estimated from five independent simulated Januaries. Units are 10^9 kg s^{-1} . Positive values correspond to counterclockwise circulation and negative values to clockwise circulation in this meridional plane.

by Julian and Chervin (1978). The second experiment (cold temperatures/no gradient, Case CTNG) imposed a zero OST zonal gradient by extending the local minimum values near the South American coast westward within the tropical band to 150°E . In effect, this prescribed change not only eliminates the zonal OST gradient, but also puts cooler than normal values in the central Pacific and much cooler than normal OST in the western Pacific.

In the previously described two prescribed changes, the mean OST in the latitudinal band was either raised or lowered, thereby creating energy sources or sinks relative to the control. In order to evaluate the effect of a zero zonal gradient in OST without the influences of additional energy sources or sinks, the sector mean OST values for each latitude line in the band were imposed at all points on the line. This experiment (mean temperatures/no gradient, Case MTNG) therefore features a modest warm anomaly near the South American coast and a modest cold anomaly west of the date line.

The position of South America immediately to the east of the downward branch of the Pacific clockwise Walker cell very likely influences the characteristics of that zonal circulation. The vigorous convection, prevalent over continental longitudes throughout the tropics, moves mass aloft, contributing to the momentum of connecting zonal winds in the upper troposphere. In order to consider the role of the South American continent in the simulated Walker circulation, a fourth experiment (no South American continent, Case NSAC) was performed which considered the entire South American surface area as if it were ocean. Ocean surface temperatures were assigned to the changed grid boxes by interpolating the climatological values from west to east between the Pacific and Atlantic coastal waters. Other grid boxes retained their climatological OST as in the control ensemble.

In the following sections, we assess the impact of these four independent prescribed changes in terms of changes in zonal wind, vertical velocity, streamfunction and surface energy and moisture balances. It is hoped that the consideration of all the prescribed change responses for a particular field or variable at once will present a relatively clear picture of the relative influence of OST gradient and continentality on the overall structure of Walker circulation and the intensity of the various cells.

4. Tropical response

In Section 2 we defined the model's Walker circulation in terms of longitude-height cross sections of zonal wind and vertical velocity averaged over the latitude band from 8°N – 16°S . Here, we present comparable cross sections for the January mean for each of the prescribed change experiments as well as

difference cross sections in which the control ensemble average is subtracted from the January mean for each case. Statistically significant differences (at the 5% level) are shown stippled on the prescribed change response (Δ) cross sections.

a. Zonal wind

Figures 3 and 4 show for the latitude band under consideration the zonal wind January means and prescribed change responses, respectively, for all four experiments. Typically, there are statistically significant changes in the intensity of several cells both within and outside the region of the prescribed changes. In some cases, massive disruption of the six-cell structure (from the control) results.

In Case WTNG, the OST anomaly has weakened the zonal winds over the Pacific Ocean, almost completely stalling the Pacific cell. The easterly trade winds have been replaced by weak westerlies, but the average is close to zero over wide expanses. Bjerknes (1969) and later Newell *et al.* (1974) related the strength of the easterly surface winds over the equatorial Pacific to the zonal pressure gradient and therefore supposed that the flow is regulated by the east-west OST gradient. In support of this reasoning, they showed that during seasons of anomalously warm OST in the eastern tropical Pacific (and therefore small OST zonal gradient), the Walker circulation (i.e., our Pacific cell) was slowed (e.g., during the period December 1963–February 1964). Although it has been pointed out that such warming can also be a consequence of weakened trade winds, the WTNG results emphasize the positive feedback whereby an El Niño warm OST anomaly inhibits the normal Pacific cell in the Walker circulation. The use of prescribed OST in the model simulations, of course, precludes any evaluation of the feedbacks involving atmospheric effects on OST. The downstream response which results in a significant intensification and broadening of the Atlantic and Indian cells has the appearance of a compensation for the weakening of the Pacific cell. Except in a relative (to the zonal average) sense, the South American and African cells disappear. Consequently, the entire structure of the global Walker circulation is significantly altered in this case.

In contrast, Case CTNG shows a significant intensification of the Pacific cell with a westward shift of the upper level westerly core from 115°W to 165°E . It will be shown below that this intensification also finds a parallel in observations. Compensations in the zonal plane include a significant weakening of the upper level of the Atlantic cell and a weakening and considerable narrowing of the maritime cell. This latter cell is essentially eliminated. Later it will be shown that the vertical velocity changes for this case are equally dramatic with the concentration of con-

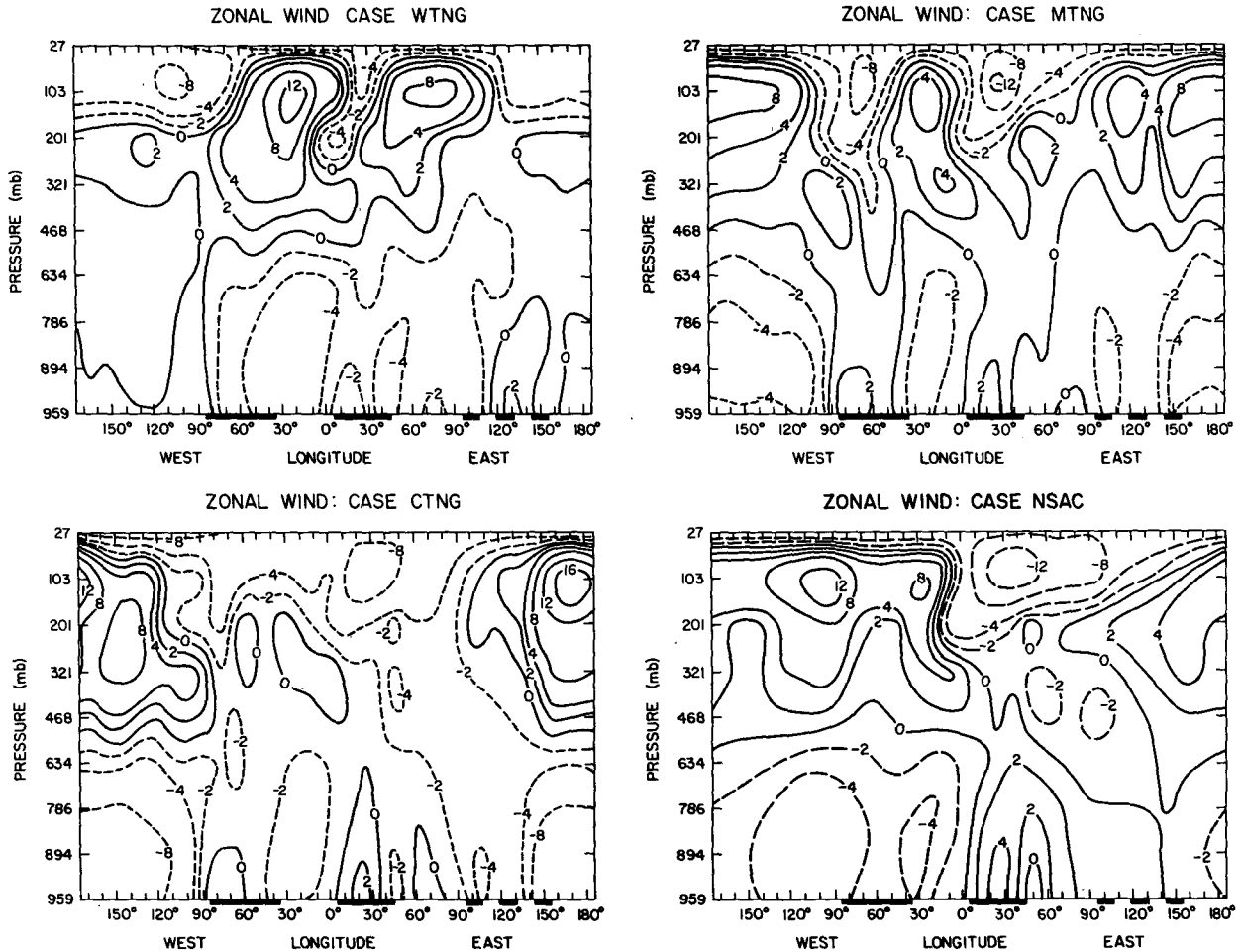


FIG. 3. Longitude-height January mean cross sections of the zonal wind for each prescribed change experiment averaged over the latitude band 8°N – 16°S : upper left, warm temperature, no gradient case (Case WTNG); lower left, cold temperature, no gradient case (Case CTNG); upper right, mean temperature, no gradient case (Case MTNG); lower right, no South American continent case (Case NSAC). The solid underbars indicate the South American and African continents and the broken underbar indicates the maritime continent formed by the Indonesian Archipelago and New Guinea. Units are m s^{-1} .

vective activity over the maritime continent as the primary influence.

The Case MTNG response appears to be a blend of the responses found in the previous two cases. This result should not be too surprising since this prescribed change consists of a cold OST anomaly in the west and a warm anomaly in the east. The Pacific cell is significantly intensified in the western part and weakened over the eastern tropical Pacific. Also, as in Case CTNG, the western edge shifts westward and eliminates the weak maritime cell. The downstream response is mostly insignificant. Some possible exceptions are the slight weakening of the Atlantic and African cells. These results lend support to the argument that the OST zonal gradient is not the primary driving mechanism of the Walker circulation, especially for the dominant Pacific cell.

The removal of the South American continent in Case NSAC produced substantial differences in the

overall structure of the zonal wind. The counterclockwise South American cell disappears as the upper level westerlies and the lower level easterlies of the Pacific cell shift eastward to include the region above the former position of the continent and merge with the respective components of the Atlantic cell. In fact, the simulated Walker circulation nearly becomes a two-cell system as the African counterclockwise cell becomes stronger and broadens, practically eliminating the Indian cell.

b. Vertical velocity

The vertical velocity means and differences shown in Figs. 5 and 6, respectively, largely conform to the patterns and responses previously discussed for the zonal wind. This conformity indicates that to a considerable degree the model's Walker circulation is confined to the two-dimensional longitude-height

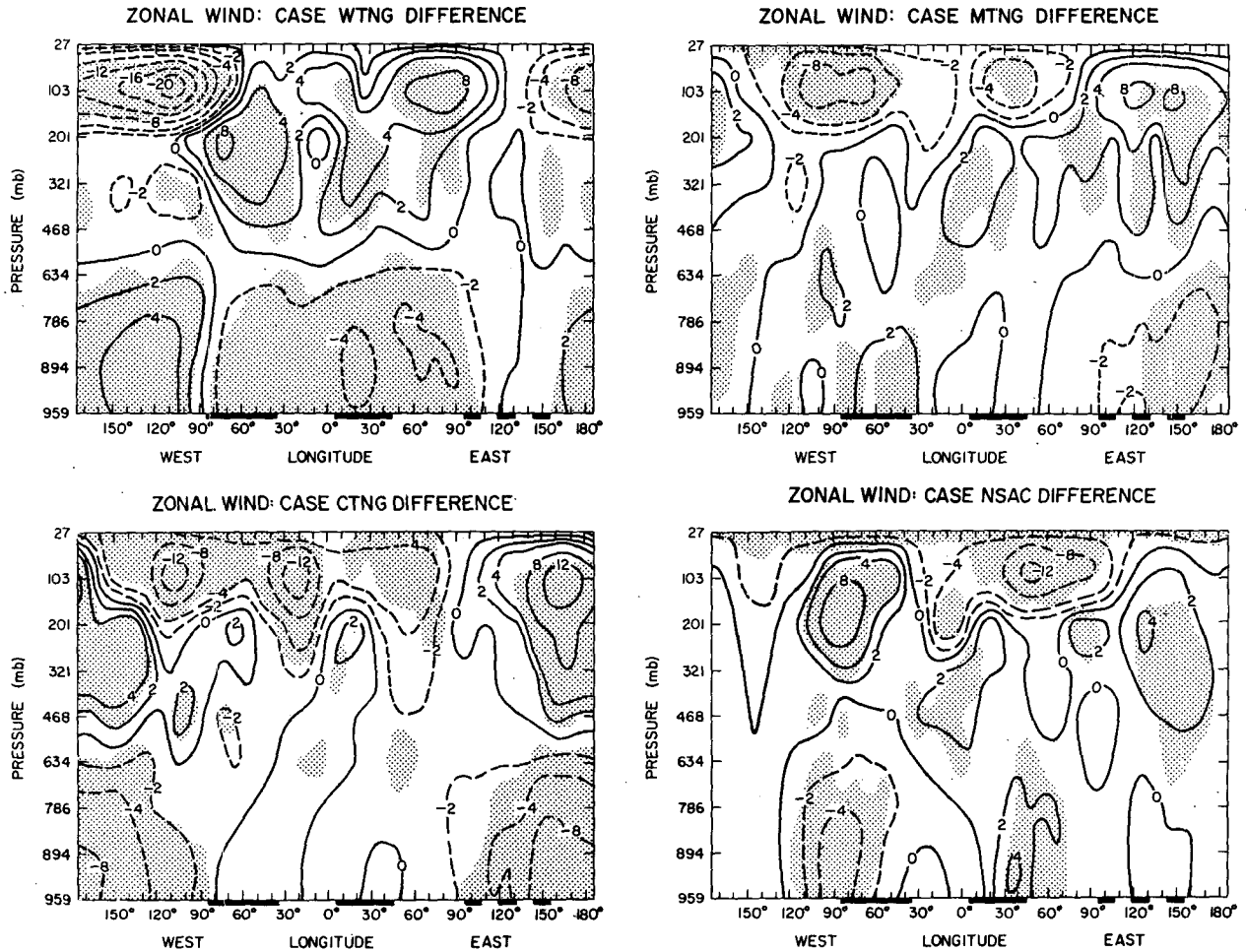


FIG. 4. As in Fig. 3 except for prescribed change responses, i.e., the control ensemble average as estimated from five simulated Januaries is subtracted from the January mean for each experiment. Stippled areas correspond to normalized responses $r \geq 3$ and indicate statistically significant differences at the 5% significance level. Units are m s^{-1} .

plane. There are, however, some extratropical interactions, as will be discussed in the next section.

In Case WTNG, the downward branch of the Pacific cell has been replaced by convection, thereby creating a broad area of upward motion which now extends from the maritime continent eastward to 30°W . Consistent with a previously demonstrated weakening of the Pacific cell, the upward motion over the maritime continent and the western Pacific is generally reduced. There are also significant changes in the structure of the upward branches over South America and Africa with the maxima occurring at higher levels in Case WTNG and being of larger magnitude. For the December 1963–February 1964 El Niño episode, Newell *et al.* (1974) also showed a cessation of subsidence over the warm OST anomaly.

The usual convection over the central and western Pacific Ocean has been considerably reduced in Case CTNG. In compensation, however, upward motions have become concentrated over 140°E , just to the

west of the most anomalous OST. Unlike Case WTNG in which the boundary layer thermal forcing over South America adjacent to the OST anomaly inhibited compensating downward vertical motions, here warm OST and some continentality (New Guinea) are conducive to thermal convection, and the upward branch of the Pacific cell is shifted westward and is considerably intensified. Additionally, the pattern of upward motion now extends even farther to the west, eliminating all subsidence over the remainder of the Eastern Hemisphere—except in the vicinity of 60°E . The longitudinally continuous upward motion over Indonesia is perhaps responsible for the disappearance of the surface westerlies in this simulation and the slowing of the overlying easterly flow. A redistribution of the maxima in the South American and African upward branches occurs as in Case WTNG.

The prescribed conditions of Case CTNG are similar to those of December 1962–February 1963 during which time anomalously cold water was observed in

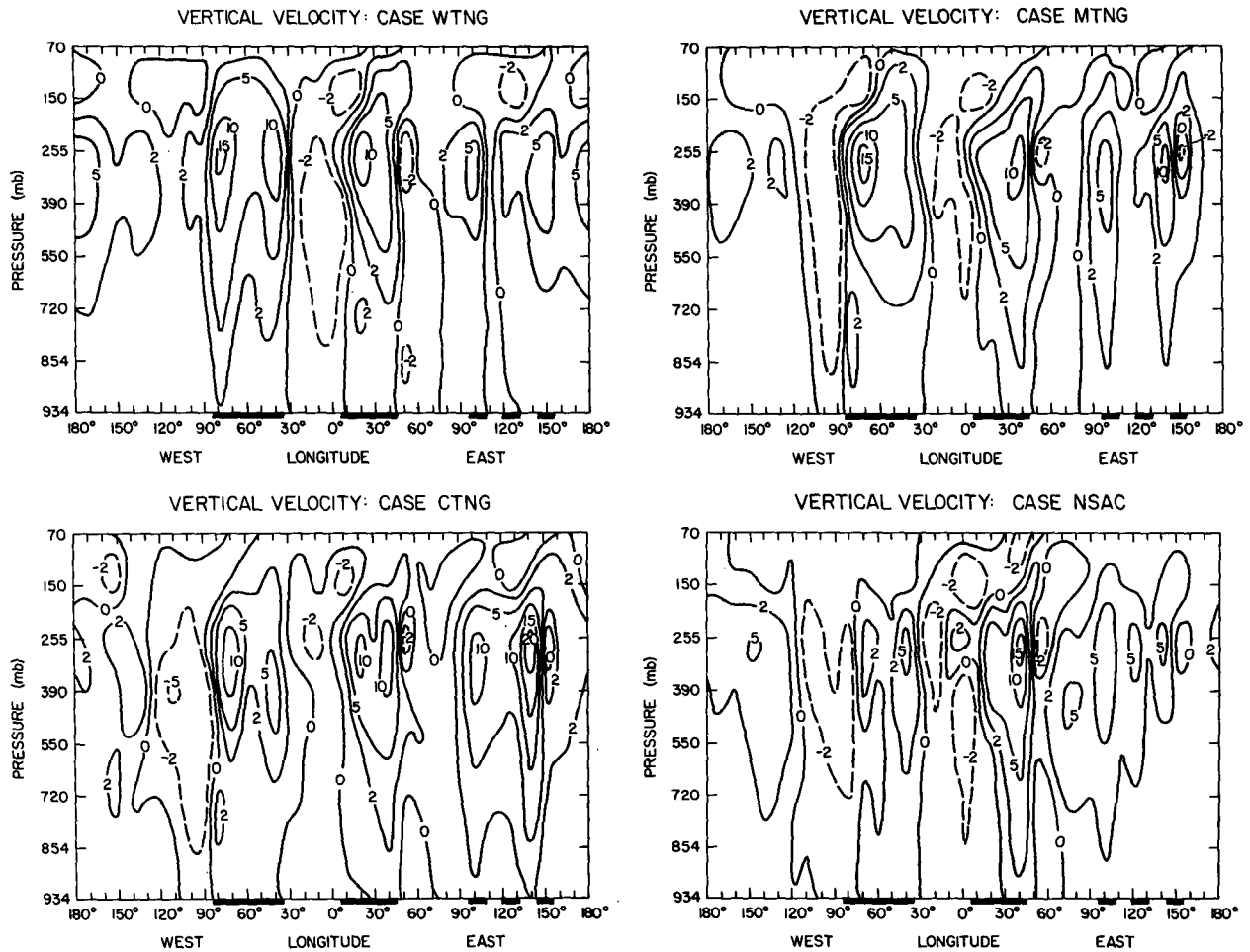


FIG. 5. As in Fig. 3 except for vertical velocity. Units are mm s^{-1} .

the central and eastern tropical Pacific Ocean. In their analysis of the atmospheric conditions corresponding to this cold episode, Newell *et al.* (1974) describe a relatively strong Pacific cell with a much broadened area of subsidence over the eastern Pacific, a broad area of rising motion over the western Pacific and Indian Ocean and rather strong easterly Pacific Ocean winds in the lower troposphere. These characteristics (with the exception of the broadened area of subsidence) were all reproduced to a considerable degree by the model. However, we can safely assume that the actual conditions included a strong OST zonal gradient over the western half of the tropical Pacific; the model experiment, however, featured a prescribed zero gradient there. On the other hand, the Case CTNG response was undoubtedly influenced by a rather large surface temperature gradient near 150°E . This simulation implies that a strong Pacific cell component of the Walker circulation can occur even in the absence of a zonal OST gradient in this region. The differential vertical motion manifestation of the Pacific cell in Case CTNG could still be a consequence

of a differential latent heat release due to a convergence of moisture over the western region—the driving mechanism suggested by Cornejo-Garrido and Stone (1977).

In Case MTNG, the previously broad area of subsidence over the eastern part of the Pacific sector was somewhat narrowed and weakened while the ascending motion over the western part was also diminished in strength. This response, of course, reflects the thermal forcing of the OST anomalies. The westward shift of the ascending branch of the Pacific cell is again a reflection of the westward displacement of convection to the area of warm waters and land near 140°E , as in Case CTNG. As was shown earlier, the maintenance of strong zonal winds in the Pacific cell is also similar to Case CTNG and is perhaps related to the broadening of convection over the maritime continent necessitating a strong inflow from below and outflow aloft. Also, the surface westerlies disappeared as the maritime continent became dominated by ascending motions. Over South America and Africa an upward displacement of the

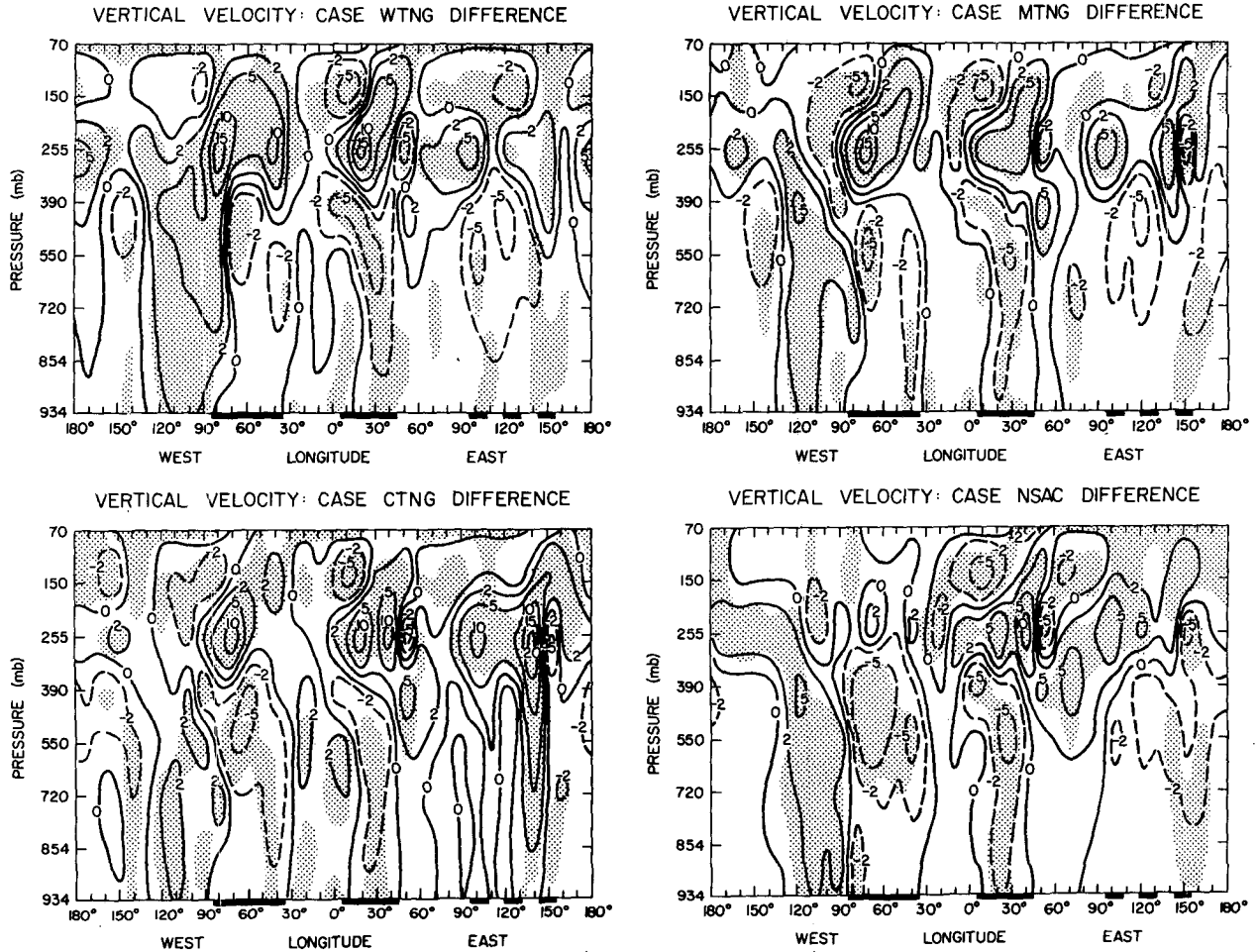


FIG. 6. As in Fig. 4 except for vertical velocity. Units are mm s^{-1} .

vertical velocity maxima is found as in the previous two cases.

Subsidence is still apparent over the eastern Pacific Ocean in Case NSAC, but is significantly weaker than in the control; it has also spread eastward over the missing continent displacing the normally encountered maximum updraft from the center of the land mass at 70°W to 40°W in a much weakened form. A significant increase in the form of a redistribution of the maximum in the upward branch over Africa occurs as a compensatory effect.

A simple categorization of the Pacific cell and its sensitivity to the various prescribed changes is possible by considering a regional and vertical average of the vertical velocity field for equally sized regions corresponding to the subsiding branch in the east and (part of) the ascending branch immediately to the west. The two regions selected for this purpose, designated central tropical and eastern tropical, each contain 15 model grid points within the latitude band of interest and are bounded by 8°N – 16°S and 175 – 135°W and by 8°N – 16°S and 125 – 85°W , respec-

tively. The results of this averaging process are shown in Table 1 in which m_c represents the estimated ensemble average for the control case, σ_c is the estimated standard deviation for the control case, m_e is the January mean for each of the prescribed change experiments and Δ is the prescribed change response (i.e., $m_e - m_c$) for each experiment. The normalized response Δ/σ_c is also included to determine the statistical significance of the differences. As before, a normalized response ≥ 3 implies significance at the 5% level.

From Table 1, it is clear that no significant changes are found for the ascending branch \bar{W}_{CT} although the upward motion is reduced considerably in Cases CTNG and MTNG, as expected. However, all four cases demonstrate significantly reduced subsidence over the eastern tropical Pacific region with \bar{W}_{ET} for Case WTNG being converted into an ascending branch. The weakening of subsidence in Case CTNG implies that the normal descent over the eastern tropical Pacific Ocean is not totally maintained by the underlying pool of cold water. This vertical

TABLE 1. January mean vertically averaged vertical velocity (0.1 mm s^{-1}).

Case	m_c	Δ	Δ/σ_c
Central tropical Pacific region (\bar{W}_{CT}) (8°N – 16°S , 175 – 135°W) $m_c = 17.9$, $\sigma_c = 4.1$			
WTNG	20.8	2.9	0.7
CTNG	11.0	-6.9	-1.7
MTNG	11.8	-6.1	-1.5
NSAC	20.0	2.1	0.5
Eastern tropical Pacific region (\bar{W}_{ET}) (8°N – 16°S , 125 – 85°W) $m_c = -24.8$, $\sigma_c = 1.6$			
WTNG	10.8	35.6	22.3
CTNG	-18.5	6.3	3.9
MTNG	-11.8	13.0	8.1
NSAC	-7.0	17.6	11.1

motion is the downward branch of broad zonal cells which apparently are driven substantially by nonlocal forces.

A logical measure of the Pacific cell "strength" is obtained by subtracting \bar{W}_{ET} from \bar{W}_{CT} and is shown in Table 2 with the same symbol conventions as in Table 1. This measure shows a significant reduction in the strength of the Pacific cell for all cases except Case CTNG where the circulation has been only marginally weakened. As is obvious from Table 1, most of the reduced strength is due to the diminished subsidence over the eastern tropical Pacific region.

c. Pacific regional energy and moisture budgets

We assessed the impact of these prescribed changes in boundary and surface conditions on the model's energy and moisture budgets for the same two regions discussed above. The results of these calculations are shown in Tables 3 and 4 for the surface energy and moisture budgets, respectively. The symbol conventions are as in Table 1.

For the cases in which the OST distributions were altered, the expected first-order response of the atmosphere to these OST anomalies was a negative feedback attempting to eliminate the anomalies. In this feedback it was also expected that altered latent heat flux from the surface would be a major influence on the surface energy balance (e.g., see Julian and Chervin, 1978). However, as is clear from Table 3, these expectations are not borne out by the experiments. In fact, the only significant change in the net heating of the surface is found in the central region for Case CTNG, and the sign of this change is counter to first-order intuition. The fallacy of the simple first-order approach is that it neglects any possible changes in the low-level winds of the Pacific cell due to the prescribed changes in OST. As was demonstrated

earlier, significant changes in the low-level winds occurred in these regions when the OST gradient was removed. The intensification of the easterlies of the Pacific cell is the likely contributor to the increase in latent heat flux in the central region for Case CTNG. Furthermore, the increase in cloudiness (see Table 4) reduced the incident insolation for this region and was thus another major factor in the reduction in net surface heating.

The most striking result shown in Table 4 is the significant increase in precipitation for the eastern region for all four prescribed change experiments. In each instance, the local evaporation change in the eastern region is not sufficient to account for all the rainfall increase. This apparent moisture deficit is actually made up by the convergence of moisture into the regions—in agreement with the conclusion of Cornejo-Garrido and Stone (1977). The total precipitation also exceeds the local evaporation for the five cases (including the control) in the central region. The largest change in total clouds found in Table 4 is in the central region for Case CTNG where the cloudiness actually increases over a cold OST anomaly. This surprising response is a consequence of enhanced vertical motion to the west of this region and the accompanying increased upper level westerly flow into the region which transports moisture and thereby creates more cloudiness. Hence, in this case, the cloud increase is caused more by advection than by convection.

The massive increase in precipitation over the eastern tropical Pacific region for Case WTNG reflects the generation of increased convection over this area instead of the usual subsidence. This result is consistent with the observations of anomalously heavy rainfall over Ecuador and Peruvian coastal stations during major El Niño events (see, e.g., Caviedes, 1975, for the 1972 event). As to be expected because of its more moderate warm OST anomaly, a lesser (though still significant) precipitation enhancement is found over the eastern region in Case MTNG.

5. Extratropical response

In this section, we primarily analyze the model's extratropical response in terms of the zonal-mean mass streamfunction. Figs. 7 and 8 show the stream-

TABLE 2. January mean Pacific cell "strength" ($\bar{W}_{CT} - \bar{W}_{ET}$) (0.1 mm s^{-1}).

Case	m_c	Δ	Δ/σ_c
$m_c = 42.7$, $\sigma_c = 4.5$			
WTNG	10.0	-32.7	-7.3
CTNG	29.5	-13.2	-2.9
MTNG	23.6	-19.1	-4.2
NSAC	27.0	-15.7	-3.5

TABLE 3. January mean surface energy budgets (W m^{-2}).

Central tropical Pacific region (8°N–16°S, 175–135°W)												
Case	Net heating [‡] $m_c = 84, \sigma_c = 7.7$			Net radiation [‡] $m_c = 212, \sigma_c = 1.6$			Sensible heat [‡] $m_c = 10, \sigma_c = 0.4$			Latent heat [‡] $m_c = 120, \sigma_c = 8.9$		
	m_e	Δ	Δ/σ_c	m_e	Δ	Δ/σ_c	m_e	Δ	Δ/σ_c	m_e	Δ	Δ/σ_c
WTNG	82	-2	-0.3	213	1	0.6	10	0	0	121	1	0.1
CTNG	52	-32	-4.2	195	-17	-10.6	3	-7	-17.5	139	19	2.1
MTNG	87	3	0.4	208	-4	-2.5	9	-1	-2.5	110	-10	-1.1
NSAC	95	11	1.4	213	1	0.6	10	0	0.7	110	-10	-1.1

Eastern tropical Pacific region (8°N–16°S, 125–85°W)												
Case	Net heating [‡] $m_c = 95, \sigma_c = 12.0$			Net radiation [‡] $m_c = 201, \sigma_c = 3.5$			Sensible heat [‡] $m_c = 11, \sigma_c = 0.5$			Latent heat [‡] $m_c = 100, \sigma_c = 7.3$		
	m_e	Δ	Δ/σ_c	m_e	Δ	Δ/σ_c	m_e	Δ	Δ/σ_c	m_e	Δ	Δ/σ_c
WTNG	70	-25	-2.1	204	3	0.9	10	-1	-2.0	121	21	2.9
CTNG	75	-20	-1.7	195	-6	-1.7	12	1	2.0	110	10	1.4
MTNG	93	-2	-0.2	208	7	2.0	11	0	0.0	109	9	1.2
NSAC	100	5	0.4	217	16	4.6	5	-6	-12.0	110	10	1.4

function January means and prescribed change responses, respectively, for all four experiments.

In Case MTNG, there is a stronger indication of polar cells in each hemisphere. However, since these changes are not statistically significant, they cannot be attributed to the prescribed changes in OST.

The slight strengthening of the Hadley cell in Case WTNG is consistent with the analysis of Newell *et al.* (1974) for a warm El Niño episode. This result is, of course, due to an increase in the zonally averaged vertical velocity. The Hadley cell in Case CTNG significantly narrows and shifts north of the equator.

TABLE 4. January mean moisture budgets.

Central tropical Pacific region (8°N–16°S, 175–135°W)										
Case	Total clouds (%) $m_c = 48, \sigma_c = 4.5$			Evaporation (mm day^{-1}) $m_c = 4.2, \sigma_c = 0.3$			Precipitation (mm day^{-1}) $m_c = 5.0, \sigma_c = 0.6$			
	m_e	Δ	Δ/σ_c	m_e	Δ	Δ/σ_c	m_e	Δ	Δ/σ_c	
WTNG	48	0.0	0.0	4.2	0.0	0.0	6.7	1.7	2.8	
CTNG	61	13	2.9	4.8	0.6	2.0	5.3	0.3	0.5	
MTNG	48	0.0	0.0	3.8	-0.4	-1.3	4.6	-0.4	-0.7	
NSAC	54	6	1.3	3.8	-0.4	-1.3	5.4	0.4	0.7	

Eastern tropical Pacific region (8°N–16°S, 125–85°W)										
Case	Total clouds (%) $m_c = 38.0, \sigma_c = 3.6$			Evaporation (mm day^{-1}) $m_c = 3.5, \sigma_c = 0.3$			Precipitation (mm day^{-1}) $m_c = 1.4, \sigma_c = 0.1$			
	m_e	Δ	Δ/σ_c	m_e	Δ	Δ/σ_c	m_e	Δ	Δ/σ_c	
WTNG	48	10	2.8	4.2	0.7	2.3	5.8	4.4	44.0	
CTNG	43	5	1.4	3.8	0.3	1.0	2.3	0.9	9.0	
MTNG	33	-5	-1.4	3.8	0.3	1.0	2.6	1.2	12.0	
NSAC	42	4	1.1	3.8	0.3	1.0	3.4	2.0	20.0	

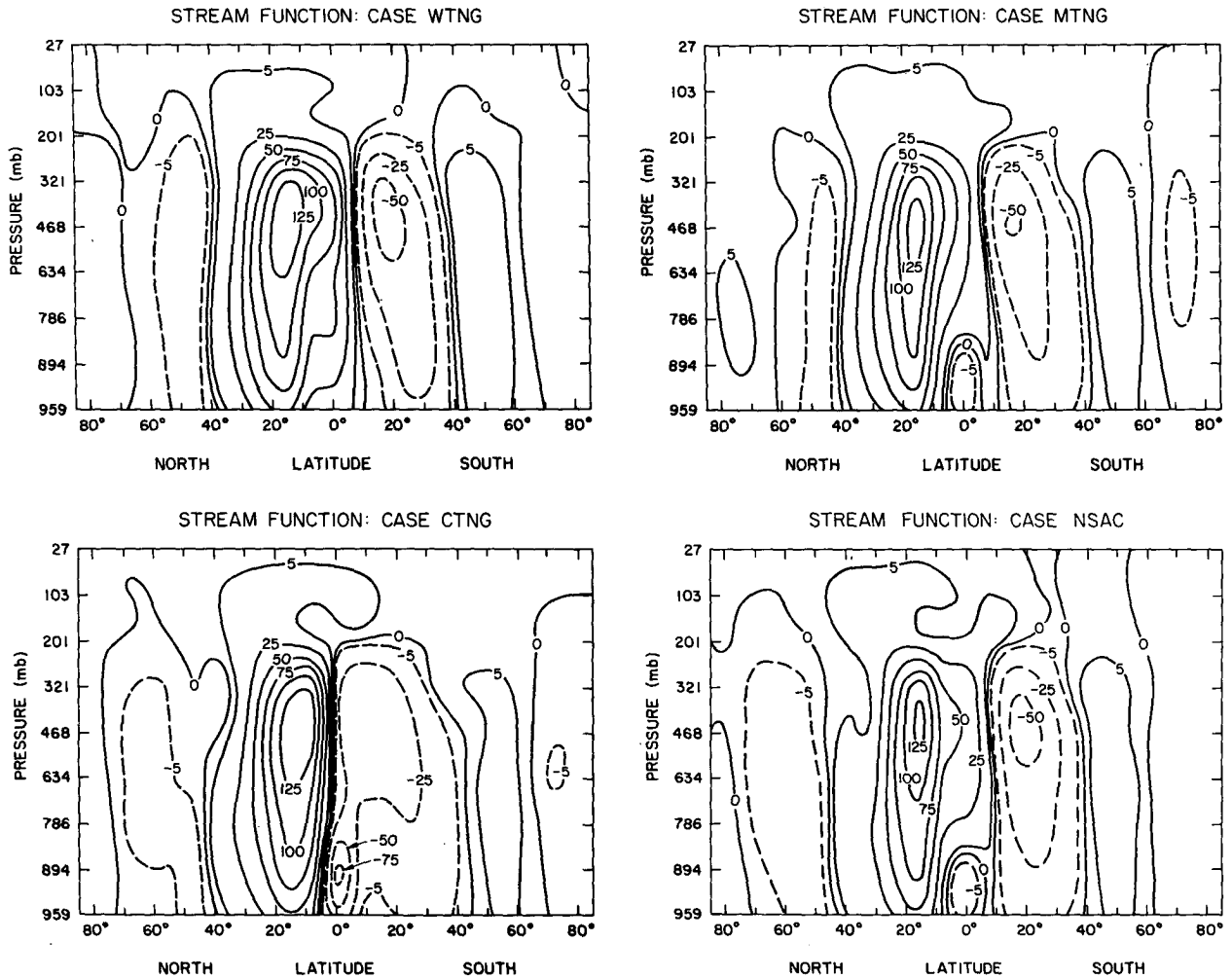


FIG. 7. The zonal-mean mass streamfunctions averaged for January for each prescribed change experiment: upper left, warm temperature, no gradient case (Case WTNG); lower left, cold temperature, no gradient case (Case CTNG); upper right, mean temperature, no gradient case (Case MTNG); lower right, no South American continent case (Case NSAC). Units are 10^9 kg s^{-1} . Positive values correspond to counterclockwise circulation and negative values to clockwise circulation in this meridional plane.

This effect probably reflects the strong upward motion over 140°E in Case CTNG. The nonconformity of this simulated Hadley cell to the one analyzed by Newell *et al.* (1974) for a cold El Niño episode is perhaps due to the rather large zonal gradient of surface land and water temperature which was imposed between 150 and 140°E . The streamfunction response in Case MTNG appears to be largely insignificant.

In Case NSAC, the Hadley cell is slightly less intense and shifted northward when compared to the control case. Obviously, the convective activity over South America contributes to both the width and intensity of the Hadley cell.

A search was also made in Case WTNG for evidence of teleconnections from the tropics to mid-

latitudes similar to those reported by Horel and Wallace (1981) from composite analyses of station data. The region around Edmonton in western Canada did have a higher surface temperature than in the control case. However, this feature was not judged statistically significant when our usual two-sided *t*-test was applied with the sample sizes available. If we could have used a one-sided test based on an *a priori* hypothesis involving a positive temperature difference for the region in question, then there would have been some marginal support in this simulation for the Horel and Wallace results. Obviously, additional model experiments of this variety would help eliminate some of the uncertainty regarding the reliability of such empirically derived relationships for surface parameters.

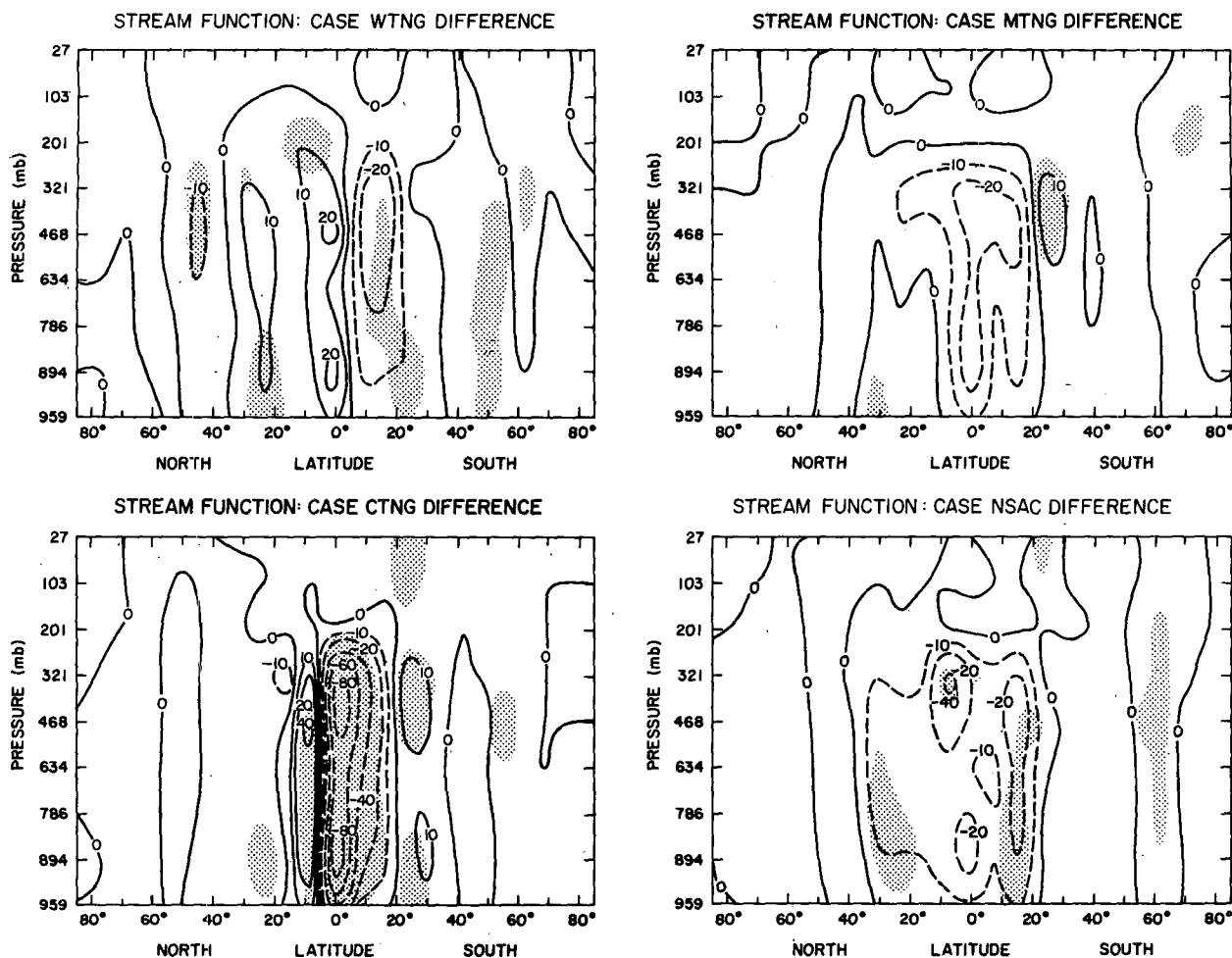


FIG. 8. As in Fig. 7 except for prescribed change responses, i.e., the control ensemble average as estimated from five simulated Januaries is subtracted from the January mean for each experiment. Stippled areas correspond to normalized response $r \geq 3$ and indicate statistically significant differences at the 5% significance level. Units are 10^9 kg s^{-1} .

6. Summary and concluding remarks

It was shown that a relatively low horizontal resolution global atmospheric model from the Goddard Institute for Space Studies (GISS) is capable of simulating many features of the observed Walker circulation during the month of January. In the model, this circulation is defined in a global sense by averaging across a latitude band from 8°N – 16°S , comprising three latitude lines of grid points. The circulation in this zonal plane may be subdivided into six distinct cells which encircle the tropics. Essentially, clockwise (when viewed from the south) cells are found over the Pacific, Atlantic and Indian Oceans. Counter clockwise cells appear over the South American, African and maritime (Indonesia to New Guinea) continents.

In an attempt to increase our understanding of the driving forces of the Walker circulation, we performed

a series of prescribed change experiments with this model in which the normal west-to-east temperature gradients in the tropical Pacific were eliminated, or the South American continent was replaced by an ocean. The purpose of these experiments was to assess the relative influence of ocean surface temperature (OST) gradient and continentality in the tropical Pacific sector on the Pacific cell in particular and the global Walker circulation in general. It was found that model simulations with a variety of imposed OST anomalies which removed the gradient differed significantly from the unperturbed control case in terms of the intensities of the different cells (both over the Pacific and downstream) that comprise the Walker circulation. The basic structure of the circulation was minimally altered for the cases in which the OST gradient was removed by replacing the normal temperature distribution either with the minimum values within the latitude band of interest or

with the sector mean values. However, major restructurings were produced by the removal of the South American continent and its associated source of convective activity and by the imposition of a large positive OST anomaly which eliminated the zonal gradient. In both cases, the counterclockwise South American cell disappeared. Thus, it appears as if the placement of the land masses within the tropical latitude band is chiefly responsible for determining the regions of ascending motion which are the foundation of the multicellular structure of the Walker circulation. The OST gradients, in turn, can play a secondary role as a modulating factor. The large positive OST anomaly experiment (featuring a net positive heat source) also indicates that an El Niño-type warming of the eastern Pacific weakens the Pacific Walker cell, not because of elimination of the zonal gradient of OST, but because of the replacement of the normal subsidence by moist convection and subsequent latent heat release over the warmed water.

For the experiment which features a warm OST anomaly in the tropical eastern Pacific, we also carefully examined the sea-level pressure and surface temperature difference fields over the North American continent for consistency with empirically derived connections from earlier observational studies. This limited sample showed a positive correlation between such OST anomalies and surface temperature in western Canada. However, the statistical significance of relationships in the model were judged marginal at best.

The extent to which the conclusions of these experiments are model-dependent is, of course, an open question. Nevertheless, the experimental results reported here can serve as a baseline for comparison with similar studies performed with other models. It would be particularly useful if these prescribed changes were imposed in models with different convective parameterizations since this physical process was identified as being a key influence in establishing the basic structure of the Walker circulation.

Also, the experimental design in these experiments may be somewhat suspect since zonal OST gradients were allowed to exist outside and at the boundaries of the specified tropical Pacific sector. These gradients may still drive the Walker circulation. Partly to alleviate this uncertainty, another set of experiments was performed with this same GISS model in which the prescribed changes were global in scope. The results of this second experimental series are reported in Stone and Chervin (1984).

Acknowledgments. We gratefully acknowledge the support and encouragement of Dr. J. Hansen and the other members of the climate research group at GISS for the use of their model and in the analysis of these experiments. Discussions with Dr. P. Stone (MIT) were most helpful in this effort. We also thank

Mrs. L.-C. Tsang of Sigma Data Services Corp. for the graphical processing of the model results. The figures were drafted and composited by the NCAR Graphics Group.

REFERENCES

- Bjerknes, J., 1969: Atmospheric teleconnections from the equatorial Pacific. *Mon. Wea. Rev.*, **97**, 163-172.
- Caviedes, C., 1975: El Niño 1972: Its climatic, ecological, human, and economic implications. *Geogr. Rev.*, **65**, 493-509.
- Chervin, R. M., 1980a: Estimates of first- and second-moment climate statistics in GCM simulated climate ensembles. *J. Atmos. Sci.*, **37**, 1889-1902.
- , 1980b: On the simulation of climate and climate change with general circulation models. *J. Atmos. Sci.*, **37**, 1903-1913.
- , and S. H. Schneider, 1976: On determining the statistical significance of climate experiments with general circulation models. *J. Atmos. Sci.*, **33**, 405-412.
- Christidis, Z. D., and J. Spar, 1981: Spherical harmonic analysis of a model-generated climatology. *Mon. Wea. Rev.*, **109**, 215-229.
- Cornejo-Garrido, A. G., and P. H. Stone, 1977: On the heat balance of the Walker circulation. *J. Atmos. Sci.*, **34**, 1155-1162.
- Drüyan, L. M., 1982a: Studies of the Indian summer monsoon with a coarse-mesh general circulation model, Part I. *J. Climatol.*, **2**, 127-139.
- , 1982b: Studies of the Indian summer monsoon with a coarse-mesh general circulation model, Part II. *J. Climatol.*, **2**, 347-355.
- Hansen, J., G. Russell, D. Rind, P. Stone, A. Lacis, S. Lebedeff, R. Ruedy and L. Travis, 1983: Efficient three-dimensional global models for climate studies: Models I and II. *Mon. Wea. Rev.*, **111**, 609-662.
- Horel, J. D., and J. M. Wallace, 1981: Planetary-scale atmospheric phenomena associated with the southern oscillation. *Mon. Wea. Rev.*, **109**, 813-829.
- Julian, P. R., and R. M. Chervin, 1978: A study of the southern oscillation and Walker circulation phenomenon. *Mon. Wea. Rev.*, **106**, 1433-1451.
- Manabe, S., J. Smagorinsky and R. F. Strickler, 1965: Simulated climatology of a general circulation model with a hydrological cycle. *Mon. Wea. Rev.*, **93**, 769-798.
- Newell, R. E., 1979: Climate and the ocean. *Amer. Sci.*, **67**, 405-416.
- , J. W. Kidson, D. G. Vincent and G. J. Boer, 1972: *The General Circulation of the Tropical Atmosphere and Interactions with Extratropical Latitudes, Vol. 1.* The M.I.T. Press, 258 pp.
- , —, — and —, 1974: *The General Circulation of the Tropical Atmosphere and Interactions with Extratropical Latitudes, Vol. 2.* The M.I.T. Press, 371 pp.
- Rowntree, P. R., 1972: The influence of tropical east Pacific Ocean temperature on the atmosphere. *Quart. J. Roy. Meteor. Soc.*, **98**, 290-321.
- Starr, V. P., J. P. Peixoto and N. E. Gaut, 1970: Momentum and zonal kinetic energy balance of the atmosphere from five years of hemispheric data. *Tellus*, **22**, 251-274.
- Stone, P. H., and R. M. Chervin, 1984: The influence of ocean surface temperature gradient and continentality on the Walker circulation. Part II: Prescribed global changes. *Mon. Wea. Rev.*, **112**, 1524-1534.
- Walker, G. T., 1923: Correlation in seasonal variations of weather VIII. *Mem. Indian Meteor. Dept.*, **24**, 75-131.
- , 1924: World weather IX. *Mem. Indian Meteor. Dept.*, **24**, 275-332.
- , 1928: World weather III. *Mem. Roy. Meteor. Soc.*, **II**, No. 17, 97-106.